Scanning Microscopy

Volume 1994
Number 8 *The Science of Biological Microanalysis*

Article 16

3-25-1994

Light Element X-Ray Microanalysis in Biology

A. T. Marshall
La Trobe University, Australia

Scanning Microscopy Supplement 8, 1994 (pages 187-201) 0892-953X/94$5.00+.25
Scanning Microscopy International, Chicago (AMF O'Hare), IL 60666 USA

LIGHT ELEMENT X-RAY MICROANALYSIS IN BIOLOGY

A.T. Marshall

Analytical Electron Microscopy Laboratory, School of Zoology, La Trobe University,
Bundoora, (Melbourne), Victoria 3083, Australia.
Telephone number: 03-4792250, Fax number: 03-4791551

(Received for publication September 27, 1993, and in revised form March 25, 1994)

Abstract

It is shown that both qualitative and quantitative light element X-ray microanalysis of biological samples is feasible. These analyses were carried out using ultrathin window (UTW) detectors. Quantitative analysis yields a total element analysis with H estimated by difference or "guesstimated". Comparison with calculated concentrations, or concentrations obtained by chemical analysis, shows that X-ray microanalysis of sections, by the peak to continuum ratio model, give sufficiently accurate results for biological purposes.

The measurement of O concentrations to yield water content is carried out using x-ray imaging techniques, so that the distribution of heavier elements can be spatially related to water and dry mass distribution. Similarly light element and heavy/light element ratios are readily visualised by X-ray imaging. These ratios can indicate the subcellular distribution of different molecular species e.g., nitrogenous compounds such as urates. It is possible to derive quantitative images of water distribution in both sections and bulk samples. Comparisons of the same sample type both as frozen sections and frozen bulk samples show that the water estimates obtained by the two different analytical methods are similar.

Oxygen analysis of C films at different specimen temperatures unequivocally reveals the temperature at which ice deposition on the specimen commences. This establishes safe conditions for reducing mass loss in model samples and freeze-dried sections to minimal levels and for avoiding artefactual oxygen analyses of both frozen-hydrated and freeze-dried sections.

Key Words: X-ray microanalysis, light elements, frozen-hydrated, freeze-dried, cell water, Malpighian tubules.

Introduction

The effectiveness and accuracy of light element X-ray microanalysis for application to biological investigations has been reviewed by Marshall (1984) and Marshall and Patak (1993). In recent years there have been considerable improvements in energy dispersive X-ray detector design and pulse processing. Electronic noise, which limits resolution of low energy X-ray peaks (Musket, 1986), has been reduced (Statham and Nashashibi, 1988) and there have been a variety of innovations to maintain detector performance such as detector crystal conditioning circuits. There have also been advances in data processing and correction procedures, particularly for bulk samples (Sevov *et al.*, 1989; Scott and Love, 1990; Bastin and Heijligers, 1992). These have greatly increased the feasibility of routine light element analyses.

There are now three types of energy dispersive detectors available for low Z analysis. These are, the windowless (W), the ultrathin window (UTW) and the atmospheric thin window (ATW) detectors. UTW detectors incorporate a thin aluminium foil in front of the detector crystal which is designed to act as a light shield. The shield does not support a pressure differential and its function is to exclude reflected light from thermionic electron guns or from other sources such as cathodoluminescence; light is a major source of electronic noise in W detectors. The detector crystal is thus functionally a part of the column environment of the microscope, just as with a W detector. As such it is susceptible to contamination by water vapour and hydrocarbons and to the degrading effects of high fluxes of high energy X-rays and high energy electrons. ATW detectors overcome this problem by having windows of materials which will withstand atmospheric pressure and which are partially transparent to low energy X-rays from light elements. These detectors, however, do not have the detection sensitivity of UTW detectors for light elements.

Little use has been made of light element X-ray microanalysis in biological investigations although the possibilities of light element analysis of biological

materials have been explored by means of electron energy loss spectroscopy (EELS) (Leapman and Ornberg, 1988). Quantitative analyses of oxygen, principally as a means of determining water composition in cells, have been accomplished by Marshall (1982, 1989), Marshall *et al.* (1985) and Marshall and Condron (1987) using a scanning electron microscope (SEM). The determination of cell water content can be regarded as a major benefit of the light element analysis of cells. The analysis of oxygen can lead to the computation of cell water content in both bulk samples and sections. In both cases this requires the analysis of frozen-hydrated samples.

If C, N and O can be accurately quantified then it may be possible to greatly improve quantitative procedures for all elements. In bulk samples the organic matrix composition can then be defined which permits the use of the so called ZAF correction procedures which are used extensively in materials science. In section analysis, using the continuum normalisation procedure, the matrix composition can be accurately calculated to obtain the matrix correction or G factor (Z^2/A) for the analysed sample. It may even prove possible to carry out standardless analysis of sections using the Ratio model since the total of all the elements analysed must be 100 percent, with hydrogen being ignored or "guesstimated". These possibilities have been investigated by Marshall and Patak (1993).

A further advantage of light element analysis is that in some circumstances meaningful information about the distribution of organic molecules can be obtained. General classes of molecules or even specific molecules may be identifiable from their C:N:O:S:P ratios. This approach has also been illustrated by Leapman and Ornberg (1988) using EELS.

The purpose of the present work is to illustrate the potential of light element X-ray microanalysis for biological investigations of cellular structure and function.

Methods

Instrumentation and analytical conditions

The analyses described here were carried out using either a scanning transmission electron microscope (STEM) (Jeol 1200EX) or a scanning electron microscope (SEM) (Jeol 840A). The STEM is fitted with a hard X-ray preventing aperture incorporating a Faraday cup, a VG Arga gas analyser, a specimen anticontaminator with a 5l liquid nitrogen dewar and a further large copper anticontaminator, with a 10l liquid nitrogen dewar, positioned over the ion pump and extending to the rear side of the specimen chamber. The liquid nitrogen retention time for both dewars is at least 72 hours. The anticontaminators are kept permanently cooled except for a periodic bake out (every 4-5 weeks). The column vacuum is maintained at $< 1.10^{-7}$ Torr with a water partial pressure of $< 1.10^{-8}$ Torr. Under these conditions no contamination is observable. The microscope is fitted with a Link 30 mm^2 Si(Li) UTW detector (resolution 134eV) and an AN10000 analyser. Analyses are carried out using either a carbon section holder with 25° tilt or a Gatan (626) low temperature holder with 40° tilt.

The SEM is fitted with a retractable Faraday cup, a VG Anavac gas analyser, a liquid nitrogen cooled anticontaminator in the specimen chamber and a liquid nitrogen cooled low temperature stage operating at -177°C. The microscope has a Link turreted LZ5 30 mm^2 detector (Be, UTW, W) (resolution 140 eV), inclined at 40° and with a solid state backscattered detector mounted on the end of the X-ray detector (Marshall, 1981), interfaced to an eXL analyser.

Analyses in the STEM of model samples and freeze-dried sections were carried out at 120 kV with beam currents of $0.5*10^{-9}$A (electron dose of $19*10^3$ e^-nm^{-2}) and $1*10^{-9}$ A (electron dose 2500 ke^- nm^{-2} to 125000 ke^- nm^{-2}) respectively, whereas analyses of frozen-hydrated sections were carried out at $1*10^{-10}$ A unless otherwise stated. In the SEM, model samples were analysed at 15 kV with a beam current of $0.5*10^{-10}$ A (electron dose 3.1 e^-nm^{-2}) and frozen-hydrated samples at 1.10^{-10}A. Quantitative elemental images were obtained in the STEM at a pixel resolution of 32 x 32 with a dwell time of 1 s for frozen-hydrated sections and 128 x 128 with a dwell time of 3 or 4 s per pixel for freeze-dried sections. In the SEM quantitative elemental images were obtained with a pixel resolution of 64 x 64 and a dwell time of 1 s.

Sample preparation

Various substances (Spurr's resin, gelatin, Nylon) of known composition (determined by calculation or chemical analysis) were prepared as films, or sections on films, for analysis in the STEM and prepared as polished blocks for analysis in the SEM. All samples were coated with 10 nm Al.

Malpighian tubules from the Black Field Cricket, *Teleogryllus oceanicus* were frozen by metal mirror cryofixation after incubation in a suitable physiological saline and sectioned on a Reichert FC4E cryoultramicrotome at -112°C. Sections on filmed Ni folding grids were cryotransferred to the microscope and analysed at -140°C. Other tubules were frozen in solid nitrogen (Marshall, 1987) transferred to a coating device where they were planed to produce a smooth surfaced specimen

and coated with 10 nm Al. Subsequently they were cryotransferred to the SEM and analysed at -177°C.

Frozen sections of frozen gelatine solutions, in which the water content was accurately measured by weighing, were sectioned and cryotransferred in the same way as the Malpighian tubule sections.

Quantitative procedures

STEM spectra were processed by means of the Link Quantem FLS program which applies the Hall peak to continuum method (Hall, 1971). SEM spectra were processed using the Link $\phi(\rho z)$ program which is based on the model by Bastin *et al.* (1984).

The standards used for STEM analyses were salts, Si_3N_4 particles, C film and SiO_2 film (Patak *et al.*, 1993). Commercial microprobe standards (Biorad) were used for SEM analyses except that chemically analysed aminoplastic resin (Roos and Barnard, 1984) was used as a standard for C, N, and O.

The estimation of water content and dry mass fraction from X-ray spectra was done in a number of ways. These include:

Method A. The continuum method (Hall and Gupta, 1979) with and without a shrinkage correction derived from a consideration of change in characteristic X-rays from an element before and after dehydration.

$$F_d = (W_{FD}/W_{FH}).S \quad (1)$$

where F_d is the dry mass fraction, W is the continuum intensity from the frozen-hydrated (FH) and freeze-dried (FD) section, respectively, and S is a shrinkage factor defined as:

$$S = I_{XFH}/I_{XFD} \quad (2)$$

with I_x being the characteristic intensity for element x.

The water mass fraction (F_w) is given by:

$$F_w = 1 - F_d \quad (3)$$

Method B. The measurement of the concentration of an element (C_x) in the frozen - hydrated and in the freeze - dried state (Hall, 1989; Roomans, 1990).

$$F_d = C_{XFH}/X_{XFD} \quad (4)$$

Method C. The measurement of mass in the frozen-hydrated and freeze-dried states assuming that mass is approximated by the sum of the X-ray intensities of [a] C, N and O or [b] C and O.

Table 1. Calculated oxygen and water mass fractions in solutions of gelatine.

Percentage H_2O	Percentage O
65	69
72	70
75	75
78	80
81	85
83	90

Table 2. Comparison of water mass fraction in frozen-hydrated sections of gelatine derived by different methods.

Method	Percentage H_2O
A	76
B	75
C a)	76
C b)	77
D	78
E	76

$$F_w \approx 1 - \frac{I_{OFD} + I_{CFD} + I_{NFD}}{I_{OFH} + I_{CFH} + I_{NFH}} . S \quad (5)$$

$$F_w \approx 1 - \frac{I_{OFD} + I_{CFD}}{I_{OFH} + I_{CFH}} . S \quad (6)$$

Method D. The simplifying assumption that the difference in O intensities between frozen-hydrated state and the freeze-dried state ratioed to the O intensity in the frozen-hydrated state approximates the water mass fraction.

$$F_w \approx F_o = 1 - (I_{OFD}/I_{OFH}) \quad (7)$$

Method E. The assumption that O concentration in the frozen-hydrated state (C_{OFH}) over a limited range approximates the water mass fraction.

$$F_w = C_{OFH} \quad (8)$$

This assumption is based on the calculation of O mass fraction in solutions of gelatine (Table 1).

In all the foregoing methods characteristic X-rays were corrected for film contributions to the spectra and characteristic X-ray intensities were corrected for absorption.

STEM elemental images consist of peak counts obtained by filtered least squares fitting of spectra at every pixel. These images can be easily manipulated mathematically to produce ratio images or can be normalised against a continuum image corrected for the presence of the support film and further processed with the necessary standard corrections to yield concentration images. Water content images were obtained by subtracting O images of freeze-dried sections from O images of frozen-hydrated sections, and ratioing to O images of frozen-hydrated sections. This uses the formalism of Method D.

Selected areas can be easily demarcated on any image to provide mean pixel intensities.

SEM elemental images were obtained as apparent concentration images. After static beam analyses of selected areas to obtain $\phi(\rho z)$ corrections for each element, these corrections factors were applied to every pixel in the apparent concentration images to yield images of real concentration. Percentage dry weight and water content images were obtained by applying correction factors, derived from the calculated relationship between O concentration and the protein concentration of an aqueous protein solution, to O images (Marshall, 1982).

Results

Analytical conditions

Mass loss. Mass loss was observed during STEM analyses (electron dose 9.8 $e^- nm^{-2}$) of freeze-dried sections of gelatine analysed at ambient (22°C) temperature compared with sections analysed at -140°C (Fig. 1). The mass loss was almost entirely due to a 67 percent loss of oxygen.

Analysis temperature. Avoiding the deposition of ice on frozen-hydrated and freeze-dried sections during analysis at low temperature is of critical importance when O is being analysed. The temperature at which ice was deposited on the sections was therefore investigated by the analysis of carbon films at different specimen temperatures. Analyses were made on different, but adjacent regions of film at each temperature. The results of a typical analytical run at two time intervals per temperature are shown in Fig. 2. Analyses conducted at longer time intervals than 15 minutes after a particular temperature was reached showed no increase in O counts.

In order to exclude the possibility that the source of ice at low temperature was the X-ray detector itself, the detector was retracted behind the vacuum gate valve and the presence of O demonstrated, after cooling a C film to -160°C, by electron energy loss spectroscopy using a JEOL ASEA10 serial electron energy loss spectrometer.

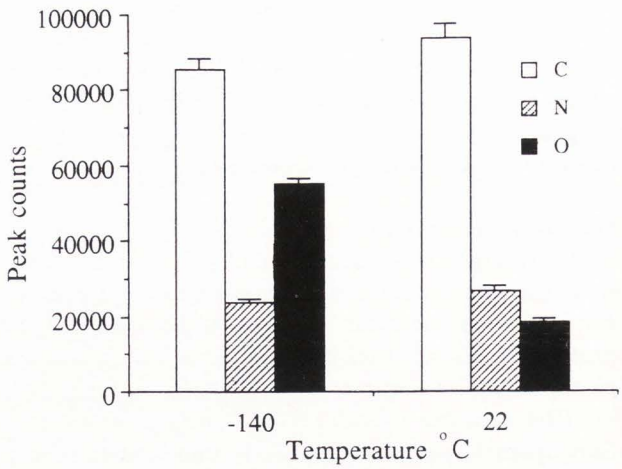

Figure 1: Compositional difference in gelatine section analysed in STEM at 22°C and -140°C.

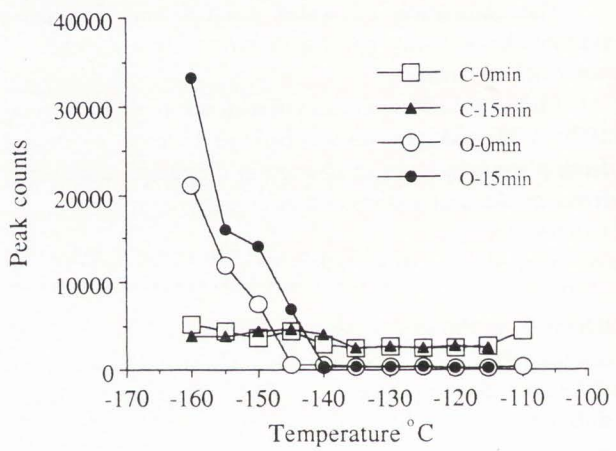

Figure 2: Graph showing change in O counts, indicative of ice deposition, from a C film analysed in STEM at low temperature.

Pulse pile up. The energy of the peak centroid for the O peak is 520 eV. There is, therefore, a risk that in frozen-hydrated samples, the very high number of counts for O will result in pulse pile up and the appearance of a spurious peak at 1040 eV which is the energy value for Na. This possibility was investigated by analyses of Formvar films on which ice had been deposited. At the count rates and dead times encountered in analyses of frozen-hydrated sections a small pile-up peak was discernable (Fig. 3a). Although small, a peak of this size converts to some tens of mmol kg^{-1} wet weight of Na. In thick Formvar films, which approximate a freeze-dried section in organic composition, pulse pile-up from O X-rays was not observed (Fig. 3b).

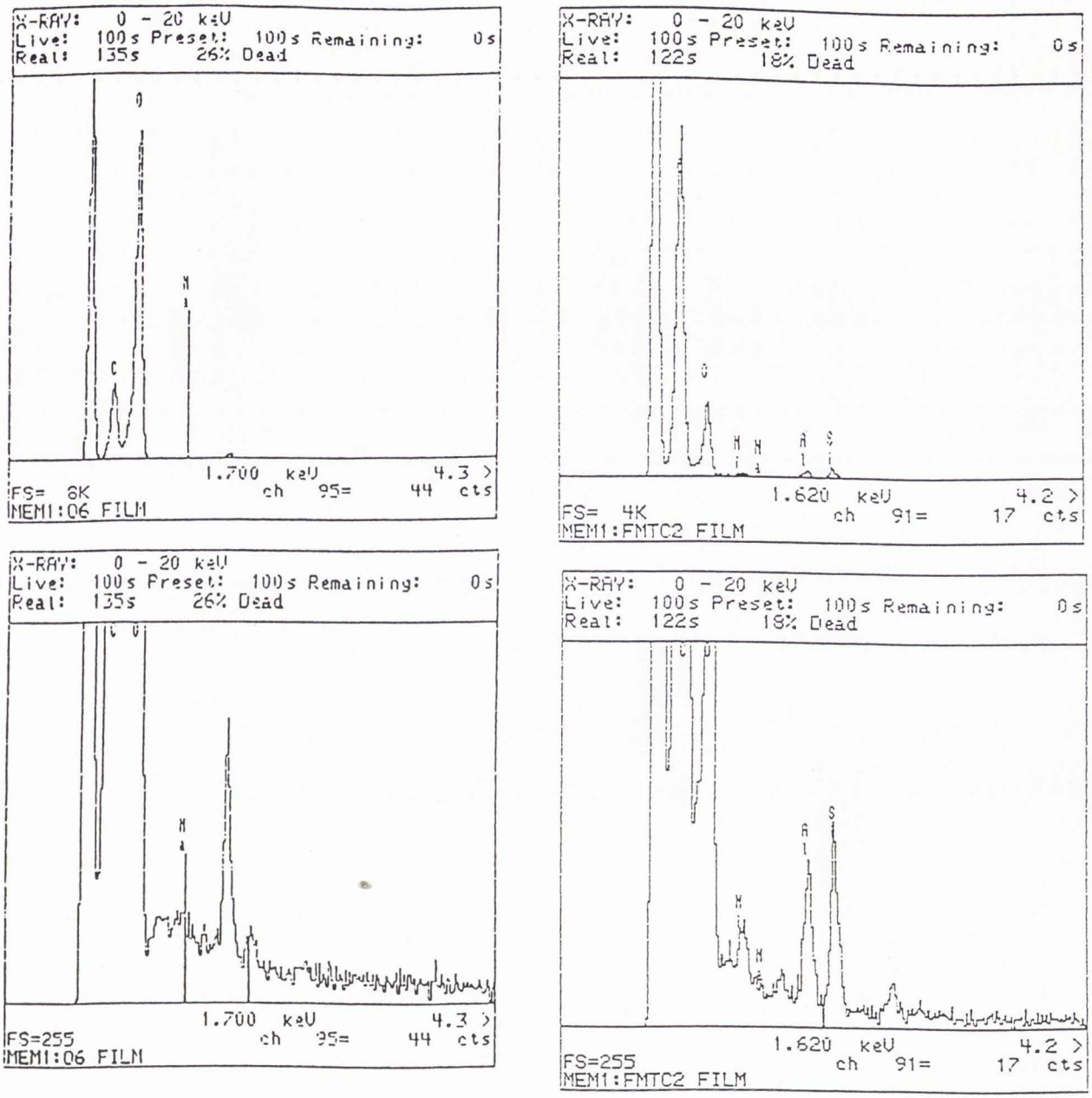

Figure 3: a) Spectra from ice b) Spectra from Formvar film.

Analysis of model systems

Films and sections of gelatin and Nylon, and sections of Spurr's resin were analysed in the STEM at -100°C using the peak to continuum model and the results normalised. Polished bulk samples were analysed in the SEM using the $\phi(\rho z)$ correction model. Comparisons of the analyses with chemical analyses of the same materials are shown in Figs. 4, 5 and 6.

Light element analysis of sections

Water content. Frozen-hydrated sections exhibit very little contrast in STEM images and are very susceptible to beam damage. Low dose, low resolution elemental images were therefore made at -139°C, following which, the section temperature was raised slowly to -100°C and held there for 15 minutes, then progressively raised by 5°C intervals, each of 15 minute duration, to -80°C at which temperature the specimen remained for 30 minutes. The temperature was then lowered to -139°C and an image made of the same area using the same conditions as previously. The images were then processed to produce an image (I_{H2O}) of

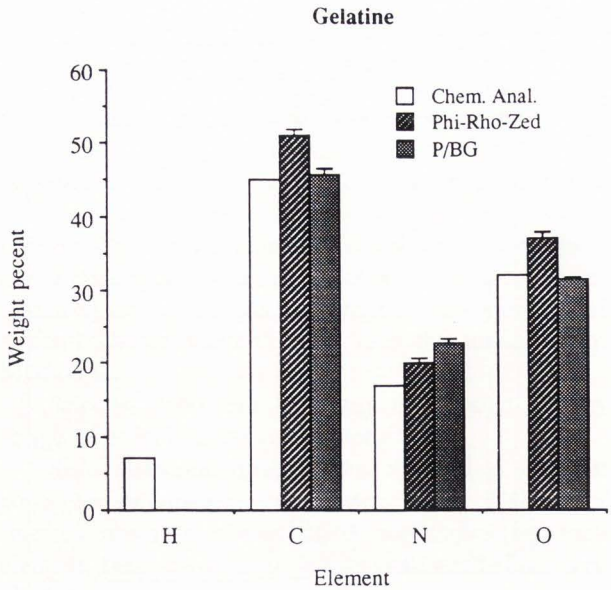

Figure 4: Comparison of gelatine analysed as films and bulk samples, in a STEM and SEM respectively, with chemical analysis.

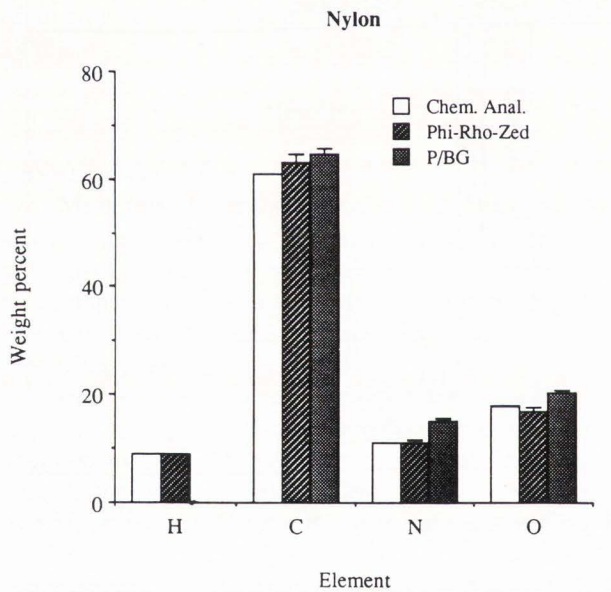

Figure 5: Comparison of Nylon analysed as films and bulk samples, in a STEM and SEM respectively, with chemical analysis.

percentage water content.

$$I_{H2O} = \frac{I_{OFH} - I_{OFD}}{I_{OFH}} \cdot 100 \qquad (9)$$

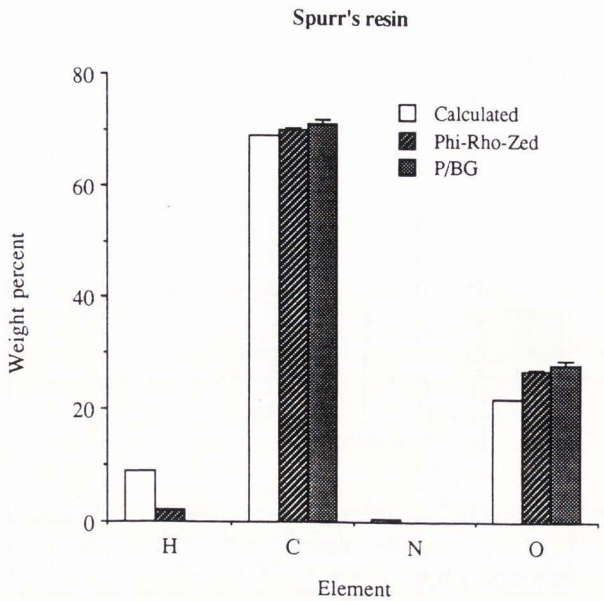

Figure 6: Comparison of Spurr's resin analysed as sections and bulk samples, in a STEM and SEM respectively, with calculated composition.

where I_{OFH} is the O image from the frozen-hydrated section and I_{OFD} is the O image from the freeze-dried section. A correction can be made for the O signal arising from the film. An analysis of this type from a section of Malpighian tubule of *T. oceanicus* is shown in Fig. 7. A selected area from which an average water content of 80.5 percent is obtained is shown.

This method of estimating water content was tested using 1 μm frozen-hydrated sections of 20% (w/v) gelatine solution in which the water fraction was measured gravimetrically to be 77% by weight. Analyses were carried out using large rasters (80 μm^2) on sections in the frozen-hydrated and freeze-dried states. The temperature regimes were as previously stated. A comparison of results obtained using the various methods of deriving the water mass fraction is given in Table 1.

The calculated total O mass fraction in the frozen-hydrated samples was 75.4% compared with a measured value of 75.8 $\pm$ 6% (n=8). In the freeze-dried sections the O mass fraction was measured to be 32.9 $\pm$ 0.8% (n=10) compared to the O mass fraction of 32% found in chemically analysed gelatine.

Distribution of C, N and O

A scanning transmission electron image of a freeze-dried section of a Malpighian tubule is shown in Fig. 8. The distribution of C and N in a cell from a freeze-dried sections of a Malpighian tubule of *T. oceanicus* is shown in Fig. 9. Within these cells the C and N peak images indicate the distribution of C and N mass. A number of

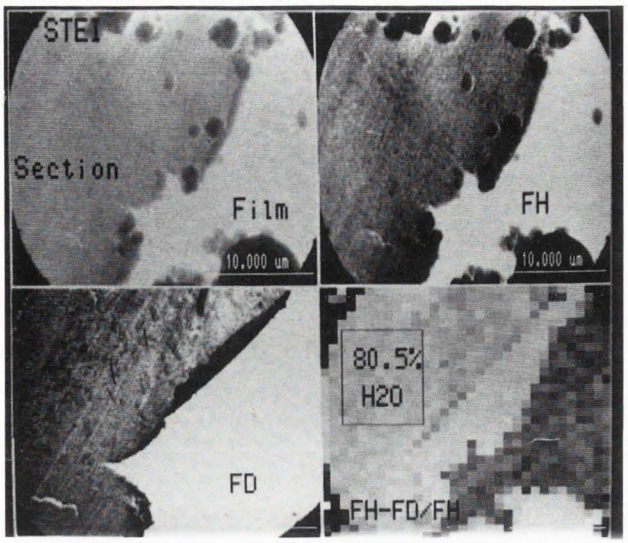

Figure 7: Oxygen analysis of frozen-hydrated and subsequently freeze-dried section of Malphigian tubule from *T. Oceanicus*. Top left is a STEM image of a frozen-hydrated section shown with increased contrast at top right.

The same section after freeze-drying in the microscope is shown bottom left and an image showing % water distribution at a resolution of 32x32 pixels is shown at bottom right. The average % water content in the boxed area is shown.

structures, including mitochondria, lysosomes, elongate organic crystalloids and nuclear heterochromatin have a high C and N mass. Ratioing N to C mass indicated the high relative N content of heterochromatin and crystalloids. Inorganic calcium phosphate containing spherites also have a high N : C ratio although they have a very low C and N mass. This ratio appears to be variable (Fig. 13).

Concentration images (Fig. 10) of C, N and O reveal further information. The C concentration in nuclear euchromatin is similar to that of heterochromatin although N concentration in heterochromatin is higher. A phosphorus concentration image (Fig. 11) shows that high concentrations of P are associated with the high N containing heterochromatin. An area of nucleus is also shown to have a high O concentration but low C and N concentrations. The O concentration in the crystalloids and lysosomes is very low with one lysosome containing P whilst the other has only very low concentrations. It is also interesting to note that the O concentration of the calcium spherites is similar to the O concentration in the general cytoplasm. It is also evident that an inclusion in the microvilli area contains Ca (Fig. 11) and C (Figs. 9, 10) but no P.

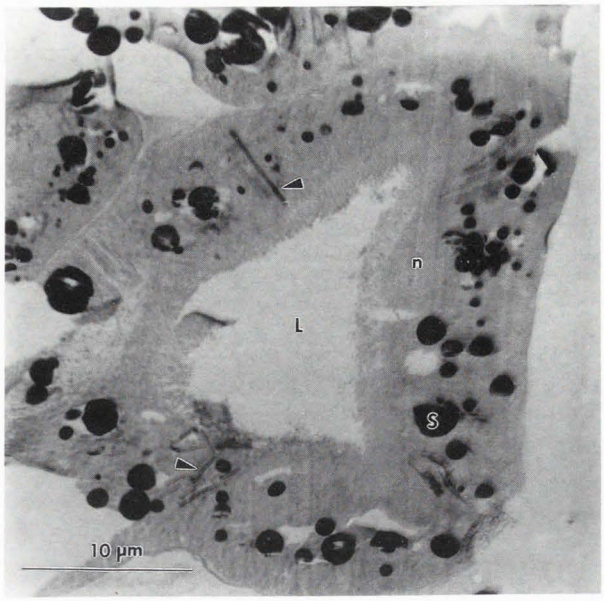

Figure 8: Freeze-dried section of Malphigian tubule of *T. oceanicus* showing lumen l, nucleus n and spherites S. Needle shaped crystals are indicated by arrows.

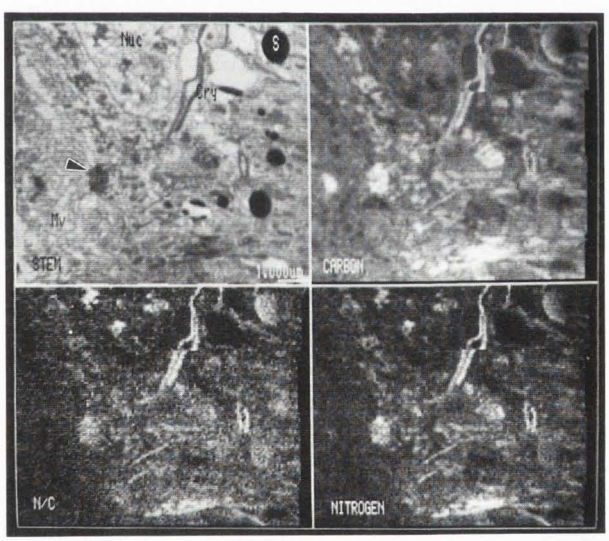

Figure 9: Peak intensity images from a freeze-dried section of Malphigian tubule cell are shown for C and N and a N/C ratio. A STEM image of the same area (top left) shows nucleus (Nuc), crystals (Cry), spherites (S), microvilli (Mv) and lysosomes (arrows).

A further example of the effectiveness of light element imaging is seen in the identification of unsuspected crystalline inclusions in Malpighian tubule cells. In Fig. 12 it can be seen from the scanning transmission electron image (STEI) that the cells contain numerous

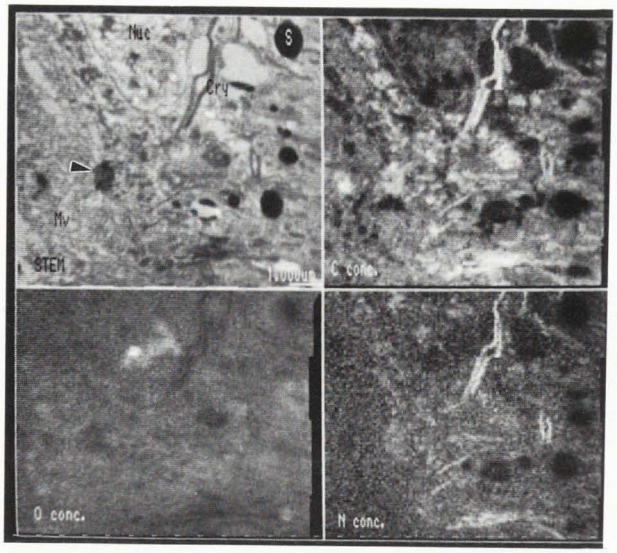

Figure 10: Concentration images from a freeze-dried section of a Malphigian tubule cell are shown for C (top left), N (bottom right) and O (bottom left). A STEM image of the same area (top right) shows nucleus (Nuc), crystals (Cry), spherites (S), microvilli (Mv) and lysosomes (arrows).

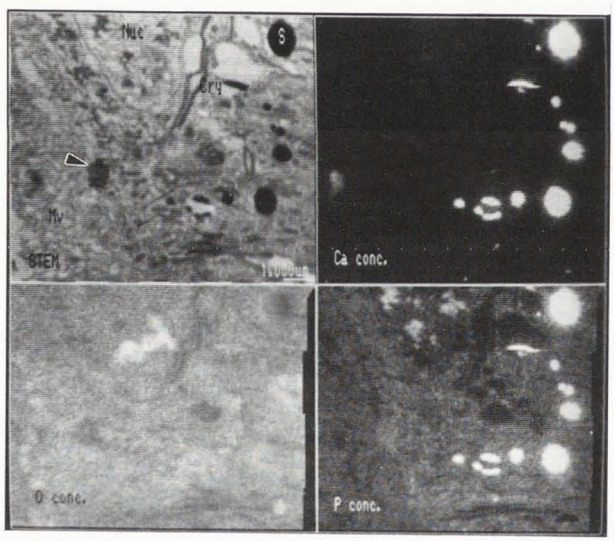

Figure 11: Concentration images from a freeze-dried section of a Malphigian tubule cell are shown for Ca (top right), P (bottom right) and O (bottom left) shows nucleus (Nuc), crystals (Cry), spherites (S), microvilli (Mv) and lysosomes (arrows).

dense spherical inclusions of calcium phosphate. Peak intensity images of C and N reveal rectangular inclusions with a high C and N mass which are not readily discerned in the STEI image or the continuum image

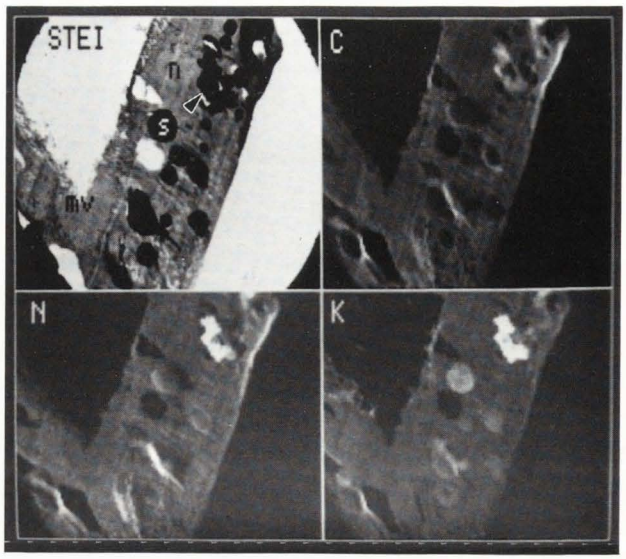

Figure 12: Peak intensity images from a freeze-dried section of a Malphigian tubule cell are shown for C (top right), K (bottom right) and N (bottom left). A STEM image of the same area (top left) shows nucleus (Nuc), microvilli (Mv) and rectangular inclusions (arrow).

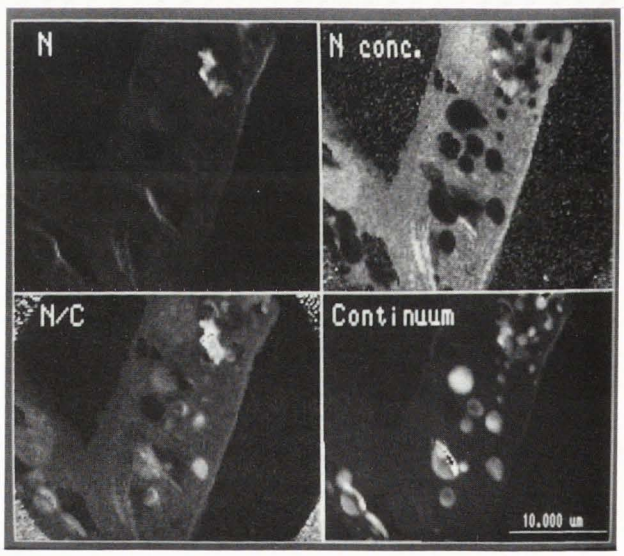

Figure 13: Comparison of images of N peak intensity (top left), N concentration (top right), continuum (bottom right) and N/C ratio (bottom left) from a freeze-dried section of a Malphigian tubule cell.

since they are obscured by spherical inclusions (Fig. 13). The C and N content of the rectangular inclusions is also correlated with a high K content. Figure 13 shows that the N concentration is high in the rectangular inclusions and the N : C ratio is also very high.

Light element analysis of bulk samples

Distribution of C, N and O. The planed surface of a frozen-hydrated bulk sample is essentially featureless in both SEM secondary electron (Fig. 14) and backscattered electron images. The distribution of the main tissue features can be obtained by qualitative X-ray imaging in a relatively short time. Some 10-20 min. was adequate to obtain a low magnification image at low resolution sufficient for orientation purposes.

Detailed quantitative images of frozen-hydrated Malpighian tubules of *T. oceanicus* show the distribution of C and O in weight percent (Fig. 14). These are obtained by applying $\phi(\rho z)$ correction factors to the apparent concentration images. A continuum image indicates the presence of intracellular calcium phosphate spherites by virtue of their higher density and average atomic number. There is an obvious correlation with regions of very low O concentrations in the O image. The high O concentrations clearly delineate the high water content of luminal contents and haemolymph, whereas the high C concentrations clearly indicated the tubule cytoplasm.

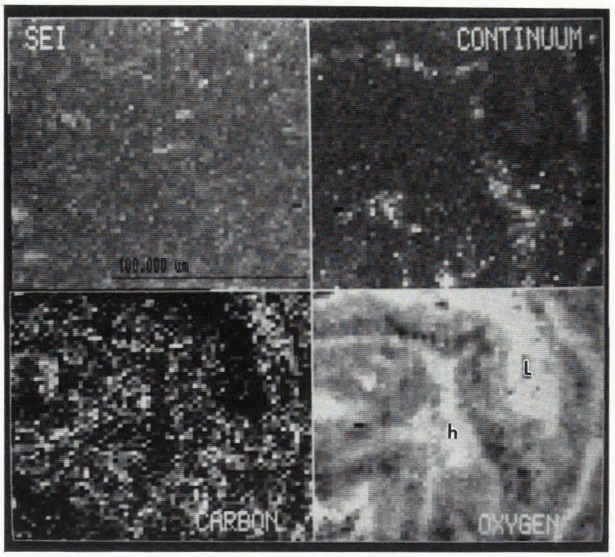

Figure 14: Comparison of continuum (top right), O peak intensity (bottom right), C peak intensity (bottom left) and secondary electron (top left) images from a frozen-hydrated bulk sample of Malpighian tubules from *T. oceanicus* (lumen-l, haemolymph-h).

Water content. Images of percentage protein or dry weight and percentage water content are obtained by applying a linear equation relating O concentration to protein concentration in an aqueous protein solution (see Table 1), to the O concentration image (Fig. 15). The percentage water image was then used to convert quantitative elemental images in mmol kg^{-1} wet weight to mmol l^{-1}. An example of this is shown for K in Figure 15. The very high luminal concentrations of K have been "sliced" out of the final image.

Oxygen concentrations can be obtained from any demarcated region. An example is shown in Fig. 16. Values obtained in this way can be easily converted to percentage water content or regions can be assessed directly from percentage water images (Table 3). In a similar manner regions of elemental concentration images in mmol l^{-1} of all water (assuming no ion binding) can be sampled (Table 4).

In Fig. 17 there are unusual differences seen in the luminal distributions of K and Cl. A possible explanation of this may be seen from the concentration image for N which indicates a weak correlation with luminal K, suggesting the possibility of concretions of potassium urate being present in the lumen.

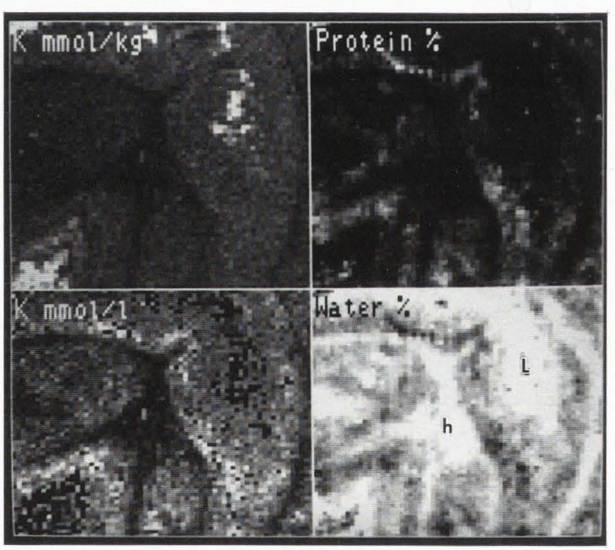

Figure 15: Comparison of derived % Protein or dry weight (top right), % water (bottom right), K concentration in mmol kg^{-1} (top left) and derived K concentration in $mmol^{-1}$ cell water (bottom left) images from a frozen-hydrated bulk sample of Malpighian tubules from *T. oceanicus* (lumen-l, haemolymph-h).

Discussion

Conditions for light element analysis of frozen hydrated and freeze-dried sections include careful selection of specimen temperature to reduce not only mass loss (principally O) but also ice deposition. Several studies using electron energy-loss spectroscopy (e.g., Lamvik, 1991) have shown that light elements are lost from organic materials during radiation. It is confirmed

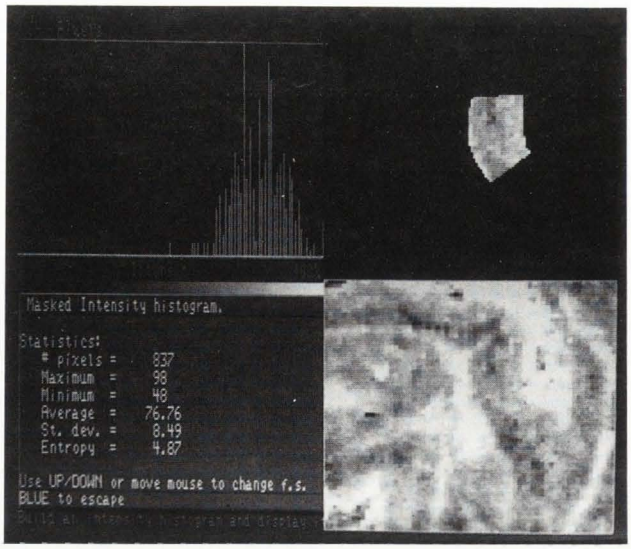

Figure 16: Isolation of a region of frozen-hydrated bulk sample of Malphigian tubules of *T. oceanicus* showing average O concentration in mmol kg^{-1} wet weight.

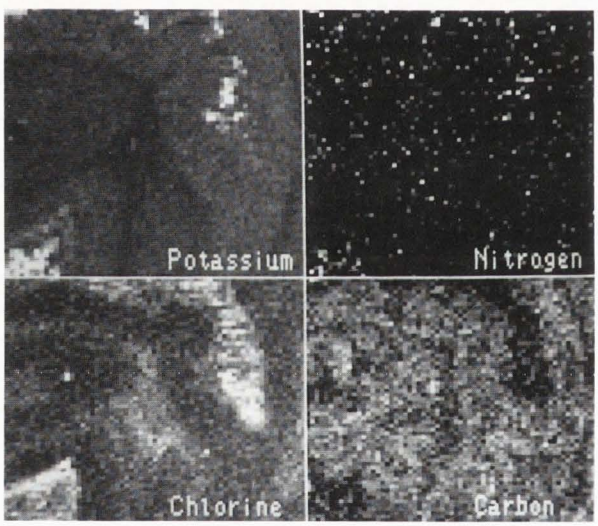

Figure 17: Concentration images (mmol kg^{-1} wet weight) of K (top left), N (top right), C (bottom right) and Cl (bottom left) from frozen-hydrated bulk samples of Malphigian tubule of *T. oceanicus*.

here by X-ray microanalysis that the principal element lost is O. This is consistent with the electron energy loss study of Leapman and Ornberg (1988). Cantino *et al.* (1986) showed by means of X-ray microanalysis that mass loss of hydrocarbons from biological samples occurred at low temperature in an erratic fashion. These authors did suggest, however, that this may have been due to the specimen being at a lower temperature than the anticontaminator with consequent trapping of water

Table 3. Water content of frozen-hydrated Malphigian tubule cells.

Tubule	Pixels/region	Percentage water
1	837	84.0±1.9
2	528	74.3±2.4
3	401	78.3±1.9
4	425	79.1±2.2

Mean±SD are given.

Table 4. Potassium concentrations in frozen-hydrated Malphigian tubule cells.

Tubule	Pixels/region	K concentration (mmol l^{-1})
1	165	227±60
2	224	227±69
3	156	292±99
4	135	296±86

Mean±SD are given.

leading to specimen etching. The question of ice deposition on the specimen does not appear to have been examined in detail previously. The present work indicates that the suggestion of Cantino *et al.* (1986) is substantially correct since the specimen temperature in the present experiments was adjusted to avoid ice deposition and the correspondence between measured and known concentrations in organic compounds precludes the occurrence of any significant mass loss.

Quantitative analysis of model samples, as reported here and by Marshall and Patak (1993) show that accurate estimates of C, N and O concentrations can be obtained in biological samples. In sections the peak to continuum model provides good results although normalisation, with the inclusion of an estimated value for H, generally improves the analysis. There is some possibility that standardless analyses, using the ratio model of Cliff and Lorimer (1975), may be feasible for section analysis (Marshall and Patak, 1993). Carbon and N analyses are particularly useful in freeze-dried sections when carried out both qualitatively and quantitatively. In frozen-hydrated sections and bulk samples quantitative O analyses are of prime interest due to the potential for estimating water content.

The estimation of water content in cells has been an area of major concern in biological X-ray microanalysis. This is due to the generally held view that a knowledge of diffusible ion concentrations in cell water is more meaningful, in terms of deciphering physiological

events, than is concentration in terms of cellular dry weight. There is no means by which X-ray microanalysis can determine ion activities and it has to be assumed, for the purposes of calculation, that no ion binding or other immobilisation of ions occurs. There is, however, a minority view that does not consider cell cytoplasm to be best described as a mixture of macromolecular structures and a solution of freely diffusible organic and inorganic substances (Ling, 1988).

Methods in current use for determining cell water content, other than measurement of oxygen concentration, include: using an internal, peripheral, standard of known elemental composition and dry mass with freeze-dried sections (Rick *et al.*, 1982); measuring the difference in continuum generation, with or without normalisation to any convenient characteristic X-ray signal, between frozen-hydrated and freeze-dried sections (Hall and Gupta, 1982); using the difference between the bright field signal from frozen-hydrated and freeze-dried sections (LeFurgey *et al.*, 1992; von Zglinicki, 1991) or the dark field signal from freeze-dried sections (Zierold, 1986) to obtain mass thickness differences; and measuring the difference in inelastic electron scattering, between frozen-hydrated and freeze-dried states, by EELS (Kopf *et al.*, 1986; Leapman and Ornberg, 1988). Of these, the peripheral standard method is not deemed suitable for high resolution analyses (Hall and Gupta, 1982), the continuum method is generally considered to require high electron doses which are damaging to thin (0.1 μm) frozen-hydrated sections and the dark field method requires standards. The bright field method can be carried out with very low electron doses but if done in a scanning transmission electron microscope (STEM) an independent calibration method must be used (LeFurgey *et al.*, 1992). Parallel EELS offers the advantages of low electron dose with no requirement for standards. It is, however, limited to thin sections. The measurement of oxygen intensities as a method for obtaining water content overcomes some of the difficulties inherent in the foregoing. It is also a more direct method which has the convenience, but not the apparent limitations, of the continuum method. It should be pointed out, however, that if the total available continuum is used (there appears to be no fundamental difficulty in doing this if the filtered least squares fitting procedure is used for processing spectra) respectable statistics are obtainable even at low electron dose. The counts so obtained are, however, still an order of magnitude lower than the O counts under the same conditions.

The method used for obtaining water mass fractions from O images i.e. Method D seems to be justified, although an approximation, since the value obtained on model samples was identical to the known value. Furthermore, values obtained by other methods were all close to the value obtained by Method D. The method should be tested over a wide range of water mass fractions in model samples. These investigations are currently in progress.

The derivation of water content from O images, as practiced so far, provides average values over a large area of cell and as such is similar to, and has similar limitations to the continuum method of Saubermann and Heyman (1987), the bright field methods of Lefurgey *et al.* (1992) and von Zglinicki (1991), and the EELS method of Leapman and Ornberg (1988). The limitation is that only an average value is obtained in the frozen-hydrated state and that determination of water content in particular compartments relies principally on mass thickness measurements in the freeze-dried section. Thus water content is determined either as:

$$\% \text{ water} = 1 - (AMT_{FD}/AMT_{FH}) \cdot 100 \qquad (10)$$

where AMT is the average mass thickness

or

$$\% \text{ water} = 1 - (SMT_{FD}/AMT_{FH}) \cdot 100 \qquad (11)$$

where SMT is the specific mass thickness

instead of

$$\% \text{ water} = 1 - (SMT_{FD}/SMT_{FH}) \qquad (12)$$

Since obtaining elemental concentrations in $mmoll^{-1}$ cell water (C_{H2O}) from the concentration in mmol kg^{-1} dry weight (C_D) is obtained from:

$$C_{H2O} = C_D \cdot \frac{100 - \% \text{ water}}{\% \text{ water}} \qquad (13)$$

the error in the estimate of C_{H2O} will increase according to the equation order $10 > 11 > 12$.

Obtaining the best estimate of % water requires that the pixels of the hydrated image are in exact register with pixels from the dehydrated image and that both images are at high resolution (128 x 128 pixels). This is very difficult to achieve due to the tendency of sections to shrink and/or move during freeze-drying. Drying sections in folding grids in the microscope column (Hagler *et al.*, 1989) results in minimal linear shrinkage but does not always prevent movement or curling of the section edges (Fig. 7). There is, however, a good possibility that high resolution, low dose, O images from frozen-hydrated and freeze-dried sections

can be obtained and kept in register. This will provide the possibility of accurate and direct determination of percentage water content of cellular compartments.

In bulk samples the derivation of water content from O concentration is less direct and depends on the assumption that the cell can be modelled by an aqueous protein solution (Marshall, 1982). Approximate as this may be there is a good correspondence between the results obtained from Malpighian tubules by this method and from frozen-hydrated and freeze-dried sections of the same specimen. The method has the merit that only a single analysis is required. The only other method of obtaining water content in bulk samples involves measuring elemental mass fractions in both frozen-hydrated and freeze-dried samples (Zs.-Nagy *et al.*, 1982), however, because of high beam penetration in the freeze-dried samples this provides rather low analytical resolution.

The small O pulse pileup peak seen at the Na X-ray energy when ice is analysed precludes the accurate analysis of Na in frozen-hydrated sections. The problem is much less for freeze-dried sections where the O count rate is considerably lower. In the analysis of frozen-hydrated bulk samples in the SEM the problem can be overcome by using the Be window in a turreted detector

The distribution and concentrations of light elements can provide interesting chemical information in spite of the fact that all cells contain numerous organic compounds with similar C, N and O content. Thus in sections of Malpighian tubules from the cricket, *T. oceanicus* two types of crystalline inclusions have been shown to contain high concentrations of N and C but low O concentrations and to have high N:C ratios. The needle-like crystals of one inclusion have no further elements associated with them whereas the other rectangular inclusion has high concentrations of K, Na and Mg. The elemental composition suggests that they may be purine-like or purine-derived compounds such as uric acid or urates. There are also indications that an apparently anomalous distribution of K in the lumen of Malpighian tubules in frozen-hydrated bulk samples may be correlated with N containing regions. This may again be indicative of the presence of K urate.

Within the nucleus the condensed heterochromatin has a higher N concentration and a higher N:C ratio than euchromatin whilst the C concentration is similar. This correlates with a higher P concentration and suggests that the DNA:protein ratio may be higher in heterochromatin than in euchromatin or, alternatively, that DNA is associated with proteins which are unusually rich in N-containing amino acid residues. An O rich body is also revealed in one particular nucleus which seems to have no distinct morphological correlate. It is not known at present whether this is of widespread occurrence.

Other interesting observations are that the mineralised, calcium and phosphorous containing, spherites in the Malphigian tubule cytoplasm have an organic content with a high N : C ratio. This also appears to be somewhat variable among spherites. Presumably this is indicative of the presence of N-rich matrix glycoproteins or glycosaminoglycans.

Conclusion

Light element analysis can be accurately carried out on frozen-hydrated and freeze-dried sections, and on bulk samples, if due attention is given to problems of mass loss and ice deposition.The prime benefit of light element analysis is the direct estimation of water content from oxygen concentrations. This method has some advantages over the alternative methods. Light element analysis can improve quantitation of other elements in both sections and bulk samples. Light element concentrations and ratios can provide useful information on the types and distribution of macromolecules within the cell.

Acknowledgements

This work was carried out with the aid of a grant from the Australian Research Council. I am indebted to Drs A. Patak, C. Farrelly and A. Wright for assistance with some aspects of this work and to L. Dalton for excellent technical assistance.

References

Bastin GF, Heijligers HJM (1992) Present and future of light element analysis with electron beam instruments. Microbeam Analysis **1**: 61-73.

Bastin GF, van Loo FJJ, Heijligers HJM (1984) An evaluation of the use of Gaussian $\phi(\rho z)$ curves in quantitative electron probe microanalysis. A new optimisation. X-Ray Spectrom **13**: 91-97.

Cantino ME, Wilkinson LE, Goddard MK, Johnson DE (1986) Beam induced mass loss in high resolution biological microanalysis. J Microsc **144:** 317-327.

Cliff G, Lorimer GW (1975) The quantitative analysis of thin specimens. J Microsc **103**: 203-207.

Hagler HK, Morris AC, Buja LM (1989) X-ray microanalysis and free calcium measurements in cultured neonatal rat ventricular myocytes. In: *Electron Probe Microanalysis* (Zierold K, Hagler HK, eds) Springer-Verlag, Berlin, pp 181-197.

Hall TA (1971) The microprobe assay of chemical elements. In: *Physical Techniques in Biological Research*

(Oster G, ed) Academic Press, New York, pp 157-175.

Hall TA (1989) Quantitative electron probe X-ray microanalysis in Biology. Scanning Microsc **3**: 461-466.

Hall TA, Gupta BL (1982) Quantification for the x-ray microanalysis of cryosections. J Microsc **126**: 333-345.

Kopf DA, LeFurgey A, Hawkey LA, Craig BL, Ingram P (1986) Mass thickness images of frozen-hydrated and freeze-dried sections. In: *Microbeam Analysis 1986* (Bailey GW, ed), San Francisco Press, San Francisco, pp 241-244.

Lamvik MK (1991) Radiation damage in dry and frozen-hydrated organic material. J Microsc **161**: 171-181.

Leapman RD, Ornberg RL (1988) Quantitative electron energy loss spectroscopy in biology. Ultramicroscopy **24**: 251-268.

LeFurgey A, Davilla SD, Kopf DA, Sommer JR, Ingram P (1992) Real-time quantitative elemental analysis and mapping: microchemical imaging in cell physiology. J Microsc **165**: 191-223.

Ling GN (1988) A physical theory of the living state: application to water and solute distribution. Scanning Microsc **2**: 899-913.

Marshall AT (1981) Simultaneous use of EDS, windowless EDS, BE and SE detectors and digital real-time line-scanning for the X-ray microanalysis of frozen-hydrated biological specimens. Scanning Electron Microsc 1981; **II**: 327-343.

Marshall AT (1982) Applications of $\phi(\rho z)$ curves and a windowless detector to the quantitative X-ray microanalysis of frozen-hydrated bulk biological specimens. Scanning Electron Microsc 1982; I: 243-260.

Marshall AT (1984) The windowless energy dispersive detector: prospects for a role in biological x-ray microanalysis. Scanning Electron Microsc 1984; II: 493-504.

Marshall AT (1987) Scanning electron microscopy and X-ray microanalysis of frozen-hydrated bulk samples. In: *Cryotechniques in Biological Electron Microscopy* (Steinbrecht RA, Zeirold K, eds) Springer Verlag, Berlin, pp 240-257.

Marshall AT (1989) Intracellular and luminal ion concentrations in sea turtle salt glands determined by x-ray microanalysis. J Comp Physiol **159**: 609-617.

Marshall AT, Condron RJ (1987) A simple method of using $\phi(\rho z)$ curves for the X-ray microanalysis of frozen-hydrated bulk biological samples. Micron Microscop Acta **18**: 23-26.

Marshall AT, Hyatt AD, Phillips JG, Condron RJ (1985) Isosmotic secretion in the avian nasal salt gland: X-ray microanalysis of luminal and intracellular ion distributions. J Comp Physiol **156**: 213-227.

Marshall AT, Patak A (1993) The use of ultra-thin window detectors for biological microanalysis. Scanning Electron Microsc **7**: 677-691.

Musket RG (1986) Considerations for application of Si(Li) detectors in analysis of sub-keV, ion-induced X-rays. Nucl Instr Methods Phys Res **B15**: 735-739.

Patak A, Wright A, Marshall AT (1993) Evaluation of several common standards for the x-ray microanalysis of thin biological specimens. J Microsc **170**: 265-273.

Rick R, Dorge A, Thuran K (1982) Quantitative analysis of electrolytes in frozen dried sections. J Microsc **125**: 239-247.

Roomans GM (1990) The Hall-method in the quantitative X-ray microanalysis of biological specimens: a review. Scanning Microsc **4**: 1055-1063.

Roos N, Barnard T (1984) Aminoplastic standards for quantitative x-ray microanalysis of thin sections of plastic-embedded biological material. Ultramicroscopy **15**: 277-286.

Saubermann AJ, Heyman RV (1987) Quantitative digital X-ray imaging using frozen hydrated and frozen dried tissue sections. J Microsc **146**: 169-182.

Scott VD, Love G (1990) The prospects of a universal correction procedure for quantitative EPMA. Scanning **12**: 193-202.

Sevov S, Degischer HP, August H-J, Wernisch J (1989) A comparison of recently developed correction procedures for electron probe microanalysis. Scanning **11**: 123-134.

Statham PJ, Nashashibi T (1988) The impact of low-noise design on X-ray microanalytical performance. In: *Microbeam Analysis 1988* (Bailey GW, ed) San Francisco Press, San Francisco, pp 50-54.

von Zglinicki T (1991) The measurement of water distribution in frozen specimens. J Microsc **161**: 149-158.

Zierold K (1986) The determination of wet weight concentrations of thin biological specimens for use in quantitative electron probe x-ray microanalysis. Scanning Electron Microsc 1986; IV: 713-724.

Zs.-Nagy I, Lustyik G, Bertoni-Freddari C (1982) Intracellular and dry mass content as measured in bulk specimens by energy-dispersive X-ray microanalysis. Tissue & Cell **14**: 47-60.

Discussion with Reviewers

R.D. Leapman: Equation 7 assumes that the oxygen intensity in the freeze-dried specimen provides a measure of dry mass. In fact, only a fraction f (about 0.2) of the dry mass is oxygen, compared with typically 0.8 for the hydrated specimen. For example, consider a compartment that is 80% water and 20% protein. If we

ignore the hydrogen atoms, approximately 80% of the mass is oxygen in the hydrated specimen but only 0.2 x 20% = 4% of the mass is oxygen in the dried specimen. The correct form of Equation 7 can be written as:

$$I_{H2O} = 1 - [I_{OFD}/f_{OFD} \cdot I_{OFH}] \cdot 100 \qquad (14)$$

where f_{OFD} is the mass fraction of O in the freeze-dried section.

Author: The foregoing is correct, although the H mass fraction should be taken into account also. Equation 5 is really a more complete and accurate formalism and also takes into account shrinkage. It is probably the negation of shrinkage and f_{OFD} which largely accounts for the success of the simplified version (equation 9) of equation (14).

R.D. Leapman: What is the estimated thickness of the hydrated cryosection imaged in Fig.7? Could it be possible that some of the oxygen X-rays are absorbed in the thicker hydrated specimen so that the O peak intensity decreases? Perhaps this could explain the anomalous water content obtained from equation 9 (corrected version).

Is it possible to estimate the water content just using X-ray spectra from the hydrated specimen? The C and N intensities would provide a measure of the dry mass fraction and O would provide a measure of the water content (after correction for the support film). This would avoid the problem of differential shrinkage when the specimen is dehydrated.

Author: The section in Fig.7 was approximately 100 nm thick. I doubt if absorption would be very significant, even in a 0.5 μm section absorption is only about 12%. In the frozen - hydrated gelatine sections corrections for absorption were made. The fact that the measured O concentration in the latter samples corresponded to the calculated concentrations seems to indicate that the absorption correction was correct. The reason why the "correct" equation gives an apparently inaccurate value is probably because shrinkage is not accounted for. It should be noted that even in the absence of lateral shrinkage there may well be a vertical shrinkage or compression.

Water content can probably be estimated over a useful range from the O concentration (equation 8) but this is fortuitous since the O concentration in a frozen-hydrated section also includes the O in the dry mass of the cell. It is the latter which precludes the approach you suggest.

W.A.P. Nicholson: As a rough approximation tissue will be 80% water of which H will be 1/9 by weight of the water, about 9% by weight of the tissue. Is it reasonable to ignore this? When you "guesstimate" the H content do you allocate it stoichiometrically to O in this way?

Author: The H content of a freeze-dried cell will approximate the H content of an average protein, say 7-10% and the H content of a hydrated cell will be 9-10%. If these mass fractions were inserted into equations 5, 6 or 7 they would more or less cancel out. Since the values are not exactly known it seems best to leave them out. For the purpose of analysing dry proteins etc as a test of quantitation, the results were improved by assuming a H content of 7% and normalising.

W.A.P. Nicholson: The pixel information was processed using either Quantem FLS or Phi-Rho-Zed on the AN10000. How long does this take for a typical 64 x 64 image?

Author: Filtered least squares fitting of reference spectra to the spectrum acquired at every pixel takes 1-3 seconds depending on the number of elements. The calculation of concentrations subsequent to acquisition requires only simple arithmetical manipulations which take a few seconds per image.

W.A.P. Nicholson: Could you estimate the relative accuracies of determining water content by the change in bremsstrahlung intensity i.e., the continuum normalisation technique and the technique measuring O content?

Author: This depends on the energy range of the continuum window. If all the continuum is used the O counts will still be an order of magnitude greater than the continuum counts. It follows from the "square root law" that the counting error will be somewhat less for the O method but it is difficult to estimate the improvement in accuracy.

B.L. Gupta: In Fig. 1 showing the mass loss at 22°C there is an apparent increase in C and N in addition to the loss of O. What is the significance of this change? Does it indicate section shrinkage?

Author: The change is not statistically significant (P=0.08).The trend is probably due to slight variations in section thickness and takeoff angle. It may also be a consequence of volume reduction (shrinkage) due to mass loss.

B.L. Gupta: What may be the source of water contamination of C film at -160°C under such high vacuum? Was the anticontamination plate not colder than the specimen? Where are the temperatures of the plate and specimen measured?

Author: Even at high vacuum with extensive liquid

nitrogen cooled traps the residual column gas is mostly water vapour. However, the source of ice deposition on the sample is almost certainly from an anticontaminator which is at a higher temperature than the sample, this is why it is important to match the "effective" temperatures of anticontaminator and sample. The microscope anticontaminator consists essentially of two concentric cylinders around the specimen, at present it is not possible to measure the temperatures of these cylinders. My estimate of their temperature is based on the temperature at which ice appears on the sample and on the observation that this temperature changes with modifications to the thermal conduction pathway between the Dewar cold finger and the anticontaminator. The specimen temperature is read from the holder immediately adjacent to the specimen position.

B.L. Gupta: For the light element analysis of sections you dried them in the electron microscope (EM) at -80°C for 30 min in the EM column. There is some evidence that a substantial fraction of cell water may not be removed unless the specimen is warmed to -30°C or higher. (Gross H 1987, In: *Cryotechniques in Biological Electron Microscopy* (Steinbrecht RA, Zierold K, eds) Springer-Verlag; Gupta BL 1989, Symp Soc exp Biol **43**: 81-110) Any comments?
Author: The actual specimen temperature may be (and probably is) higher than -80°C. Clearly some tissue components such as mucus retain a good deal of water if dried to -80°C. How significant the unremoved hydration shell water of cell proteins etc is, as a fraction of total cell water, I do not know. In most cases the procedure outlined appeared to remove all of the water expected to be present. Occasionally, this was not the case but the reason for this failure is not clear. Further experiments in this area are desirable and I shall endeavour to carry them out.

B.L. Gupta: Your Fig. 17 is a bit puzzling. It gives the impression that the K and Cl are not codistributed. Apart from the "hot spots" of K (possibly potassium urate) there seems to be much less K than Cl! Is this due to black and white prints of colour coded originals?
Author: The grey scales in the two images are not comparable. The problem is the very high counts for K in the lumen, the scale range from black to white is thus much larger than that for Cl. So low concentrations of Cl appear brighter than similar concentrations of K. These particular images were not intended for direct quantitative comparison.

B.L. Gupta: Since you get good analyses with cryosections, what is the advantage of using low resolution analyses of frozen bulk specimens?
Author: Relatively large areas can be surveyed at low analytical resolution and extracellular fluids are easier to retain in the frozen state.

B.L. Gupta: Would it be possible to do quantitative elemental mapping of something like the lateral intercellular spaces in transporting epithelia of vertebrates?
Author: It appears to be feasible in the basal infoldings of Malpighian tubule cells in freeze-dried sections. In larger intercellular spaces element migration during freeze-drying may preclude this type of analysis. If ions are associated with a polyanionic matrix in the space, as you have suggested, then maybe it would be possible.

B.L. Gupta: What is the reason for some 20-30% standard deviation (SD) values for K concentrations in Table 4?
Author: The very low count rates per pixel. The standard error (SE) values are much more impressive because of the large number of pixels averaged.